Published in final edited form as:
Neurochem Int. 2010 October ; 57(3): 248–253. doi:10.1016/j.neuint.2010.06.002.

Time course of upregulation of inflammatory mediators in the hemorrhagic brain in rats: correlation with brain edema

He Wu[a,e,*], **Zhiyi Zhang**[b,*], **Ying Li**[c,*], **Ruibo Zhao**[d], **Heng Li**[a], **Yuejia Song**[a], **Jiping Qi**[a], and **Jian Wang**[e]

[a]Department of Pathology, First Clinical Hospital, Harbin Medical University, Harbin 150001, PR China

[b]Department of Rheumatology and Immunology, First Clinical Hospital, Harbin Medical University, Harbin 150001, PR China

[c]Department of Dentistry, First Clinical Hospital, Harbin Medical University, Harbin 150001, PR China

[d]Pathology Core Laboratory, Harbin Medical University, Harbin 150086, PR China

[e]Department of Anesthesiology/Critical Care Medicine, The Johns Hopkins University, School of Medicine, Baltimore, MD, USA

Abstract

Intracerebral hemorrhage (ICH) can cause secondary brain damage through inflammation-related pathways. Thrombin and one of its receptors, protease activated receptor-1 (PAR-1); matrix metalloproteinase (MMP)-9; and aquaporin (AQP)-4 are stroke-related inflammatory mediators that have been implicated in ICH pathology. To further characterize the inflammatory response after ICH, we studied the temporal profile of the expression of these inflammatory mediators and assessed their potential correlation with brain edema formation after brain hemorrhage in rats. ICH was modeled by infusing autologous blood into the striatum. Then mRNA and protein expression was assessed over the course of 5 days. We found that the mRNA and/or protein expression of thrombin, PAR-1, AQP-4, and MMP-9 was upregulated between 2 h and 5 days after ICH. Each reached a maximal level at day 2, except for AQP-4 protein, which peaked at day 5. Brain water content after ICH presented a similar trend; it was increased at 2 h, peaked at day 2, and then decreased but remained elevated at day 5. Our data provide novel evidence that upregulation of these selected inflammatory mediators occurs very early and persists for several days after ICH, and that temporal patterns of expression of thrombin and AQP-4 are associated with brain edema formation. These findings have important implications for efforts to reduce secondary brain damage after ICH.

Keywords

Aquaporin-4; Blood; MMP-9; PAR-1; Thrombin; Intracerebral hemorrhage

Corresponding authors: He Wu: Department of Anesthesiology/Critical Care Medicine, The Johns Hopkins University, School of Medicine, 720 Rutland Ave, Traylor Bldg 809, Baltimore, MD 21205, USA Tel: 410-955-3640; Fax: 410-502-5177. wuher_2008@hotmail.com Jiping Qi: qi_jiping@hotmail.com.
*These authors contributed equally to the work

1. Introduction

Intracerebral hemorrhage (ICH) is a common and often devastating stroke subtype that frequently causes brain edema. Edema leads to an expansion of brain volume that has a severe negative impact on ICH outcomes. Inflammation has been implicated in ICH-induced brain edema formation (Wang and Doré, 2007b; Xi et al., 2006). Thrombin; one of its receptors, protease activated receptor-1 (PAR-1); matrix metalloproteinase (MMP)-9; and aquaporin (AQP)-4 are important stroke-related inflammatory mediators that might contribute to or modulate edema formation after ICH [reviewed in (Wang and Doré, 2007b; Wang and Tsirka, 2005a; Xi et al., 2003; Zador et al., 2009)].

Thrombin is released from blood clots, and through activation of PAR-1, stimulates astrocytes and microglia (Moller et al., 2000; Noorbakhsh et al., 2003) and causes neuronal death and brain edema (Lee et al., 1997; Xue and Del Bigio, 2001, 2005). Inhibition of thrombin activity reduces ICH-induced brain edema and neuronal cell death (Kitaoka et al., 2002; Xue and Del Bigio, 2005; Xue et al., 2009b). Neurotoxicity of thrombin was shown to be partially blocked by a PAR-1 antagonist (Xue et al., 2006). We have observed an increase in thrombin expression in neurons and cerebral vasculature in human brain tissue after ICH (Wu et al., 2008). Upregulation of PAR-1 protein expression has been reported in rats only in a collagenase-induced model of ICH (Zheng et al., 2009).

In addition to thrombin, other proteases, particularly MMP-9, have been suggested to be involved in ICH-induced secondary brain injury and edema formation [reviewed in (Wang and Doré, 2007b)]. Increased MMP-9 activity detected by gel zymography has been observed in rodent and human brains after ICH (Rosell et al., 2006; Rosenberg and Navratil, 1997; Tejima et al., 2007; Wang and Tsirka, 2005b; Xue et al., 2009b). Inhibition of MMP-9 activity was able to reduce ICH-induced early brain injury, edema formation, and neurologic deficits (Rosenberg and Navratil, 1997; Wang and Tsirka, 2005b; Xue et al., 2009b). Furthermore, MMP-9 was reported to act synergistically with thrombin to exacerbate ICH injury (Xue et al., 2009a).

AQPs, which belong to a family of water channel proteins, help to regulate brain water balance. AQP-4 is the most abundant isoform in the brain (Zador et al., 2009). It has been reported that AQP-4 expression is upregulated in astrocytes after ICH in rodents (Qing et al., 2009) and humans (Wu et al., 2008).

Interestingly, although thrombin, PAR-1, MMP-9, and AQP-4 have been implicated in ICH pathology, a time course of their expression, particularly within the first day after ICH, has not been established. To further our understanding of the role of inflammation in ICH pathology, we characterized the temporal profile of the expression of thrombin, PAR-1, MMP-9, and AQP-4 from 2 h to 5 days after ICH and compared their expression patterns with brain edema formation in the autologous whole-blood model in rats. The advantage of this model is that only blood is introduced into the striatum of the rat brain.

2. Experimental procedures

2.1. Animals and ICH model

All experimental protocols and procedures conformed to the guidelines of the Chinese Council for the Care and Use of Laboratory Animals and were approved by the Institutional Animal Care and Use Committee at the Harbin Medical University, China. Adequate measures were taken to ensure minimal pain or discomfort to rats. A total of 440 adult male Sprague-Dawley rats (200–250 g) were purchased from the Center for Experimental

Animals, Harbin Medical University, China. Rats were allowed free access to food and water.

The rats were anesthetized with chloral hydrate (350 mg/kg, i.p.) and then placed in a stereotaxic frame (Bilaney Consultants, Germany). A midline scalp incision was made, and a hole was drilled in the left side of the skull (3 mm lateral to the midline, 0.2 mm anterior to the bregma). Autologous whole blood (50 μL) was collected from the arteria caudilis into a needleless sterile insulin syringe without any anticoagulant. After blood collection, pressure was applied to stop the bleeding. A 26-G needle attached to the syringe was inserted stereotaxically into the left caudate nucleus (coordinates: 0.2 mm anterior, 5.5 mm ventral, and 3.0 mm lateral to the bregma). The blood was infused over 5 min, and the needle was left in place for another 5 min to minimize backflow. The syringe was then removed slowly. The hole in the skull was sealed with bone wax and the scalp was sutured. Body temperature was maintained at 37.0±0.5°C during surgery with the use of a feedback-controlled heating pad. Rats were sacrificed for analysis at 2 h, 3 h, 6 h, 10 h, 12 h, 24 h, 2 days, or 5 days after blood infusion. Control rats were infused with the same volume of saline. None of the rats died as a result of the anesthesia, surgery, or blood infusion.

2.2. Assessment of histopathology

Rats were sacrificed by an overdose of chloral hydrate and perfused transcardially with ice-cold saline. Their brains were then harvested, dehydrated, and embedded in paraffin. The brains were sliced coronally into 4-μm sections from the rostral to the caudal portion of the injection site. Three consecutive brain sections selected from the injection level and from 300 μm on each side were stained with hematoxylin and eosin for evaluation of brain damage.

2.3. Quantitative real-time reverse transcriptase polymerase chain reaction (qRT-PCR)

At 2 h, 3 h, 6 h, 12 h, 2 days, and 5 days after ICH, rats were deeply anesthetized with chloral hydrate and perfused intracardially with ice-cold, RNase-free phosphate-buffered saline. The brains were rapidly removed and dissected. The ipsilateral hemispheric brain tissue was placed in liquid nitrogen prior to RNA extraction. Total RNA was prepared with Trizol Reagent (Invitrogen, Carlsbad, CA).

PCR reactions were carried out in 96-well plates with an ABI PRISM 7300 Sequence Detection System (Applied Biosystems, Foster City, CA) using SYBR Green to monitor in real-time the amplification of the target gene. The reaction mix contained 200 nM of each primer, 5 μL cDNA (corresponding to ~3 ng DNA), and 10 μL 2 × SYBR Green Master Mix Reagent (Applied Biosystems) in a total volume of 25 μL. Aliquots from the same cDNA sample were used with all primer sets in each experiment. Reactions were run according to the manufacturer's recommended cycling parameters: 93°C for 2 min followed by 40 cycles at 93°C for 1 min and 55°C for 1 min. Each PCR reaction was completed in triplicate. Standard curves were generated from serial dilutions of cDNA standards. The mRNA level was expressed in arbitrary units. Primers used were as follows: PAR-1, 5′-TGCCTTTAAGCCCAGTAGG TG-3′ (forward) and 5′-AAGCACAAGGTCCTGGGT TC-3′ (reverse); AQP-4, 5′-AGATCAGGGTGCTCCAGTCG-3′ (forward) and 5′-TGTGCCCCTCTATTCCTGGT-3′ (reverse). Five rats per group were assessed at each time point.

2.4. Immunohistochemistry

Brain sections were de-waxed and rehydrated, rinsed with distilled water and phosphate-buffered saline, quenched with 3% H_2O_2, blocked in 10% normal goat serum, and incubated overnight at 4°C with primary antibodies: mouse anti-PAR-1 monoclonal antibody (1:100;

Santa Cruz Biotechnology, Santa Cruz, CA) and goat anti-MMP-9 polyclonal antibody (1:100; Santa Cruz). The sections were then incubated with biotinylated goat anti-mouse IgG or rabbit anti-goat IgG (1:1000; DAKO) for 1 h at room temperature, washed three times, and incubated with streptavidin-peroxidase for 30 min. Finally, the immunoreactions were visualized with diaminobenzidine-H_2O_2 solution. Sections were washed, successively dehydrated in ethanol, and defatted in xylenes. Cover slips were placed over the sections with Permount (Fisher Scientific, Pittsburgh, PA). Control sections were processed without the primary antibodies and showed no positive signals.

To quantify the number of immunoreactive cells labeled with PAR-1 or MMP-9, three sections (from the injection site and 300 μm on each side) per rat were selected, and positively stained cells were counted randomly in 10 comparable fields (magnification, × 400) adjacent to the hematoma. The numbers of immunoreactive cells from 30 locations per rat (10 fields per section × three sections per rat) were averaged and expressed as positive cells per high-power field, as previously reported (Wang and Doré, 2007a; Wang et al., 2003). Five brains per group were assessed at each time point.

2.5. Western blot analysis

Rats were deeply anesthetized and perfused transcardially with ice-cold saline before being sacrificed at different time points post-ICH. The ipsilateral hemispheric brain tissue was homogenized and the protein samples (80 μg) were separated by sodium dodecyl sulfate-polyacrylamide gel electrophoresis and transferred to a polyvinylidene fluoride membrane. After being blocked with 5% nonfat milk in Tris-buffered saline–Tween 20, membranes were probed with mouse monoclonal anti-PAR-1 (1:500, Santa Cruz), mouse monoclonal anti-AQP-4 (1:500, Santa Cruz), goat polyclonal anti-thrombin (1:100, Santa Cruz), or goat polyclonal anti-MMP-9 (1: 100, Santa Cruz) overnight at 4°C. Then membranes were incubated with a 1:7000 dilution of secondary antibody (IRDye 700DX conjugated rabbit anti-goat antibody or IRDye 800CW conjugated rabbit anti-mouse antibody, Rockland Immunochemicals, Gilbertsville, PA). The antigen-antibody complexes were visualized with the Odyssey Infrared Imaging System (LI-COR, Lincoln, Nebraska). Glyceraldehyde-3-phosphate dehydrogenase (GAPDH) was used as a protein loading standard. The relative intensities of bands were analyzed with Image-Pro Plus 6.0 (MediaCybernetics, Bethesda, MD) and values were normalized to the value of a saline-infused control animal on each gel. Each experiment was performed in triplicate. Five rats per group were assessed at each time point.

2.6. Brain water content

Brain water content was determined by the wet/dry weight ratio method. Rats were euthanized by an overdose of chloral hydrate. After the olfactory bulbs, brain stem, and cerebellum were removed, the rest of the brain was immediately weighed on an electronic analytical balance (Changzhou Instruments, Inc., Changzhou, China) to obtain the wet weight and then dried at 100°C for 24 h in an Electric Blast Drying Oven (Chongqing Sida Apparatus, Inc, Chongqing ,China) to obtain the dry weight. Brain water content was expressed as (wet weight – dry weight)/wet weight of brain tissue ×100. Five rats per group were assessed at each time point.

2.7. Statistical analysis

All data are reported as mean ± standard deviation (SD). The statistical significance of the data was determined by analysis of variance (ANOVA) and post hoc tests. The correlation between brain water content and target protein expression was analyzed by Spearman correlation test with SPSS 13.0 for Windows (SPSS Inc, Chicago, IL). $P < 0.05$ was regarded as statistically significant.

3. Results

3.1. Histopathologic findings

The blood model in rats produces hematoma mostly restricted to the caudate nucleus. We observed a few scattered neutrophils in the perihematomal area at 3 h. Tissue necrosis was not evident at this time. Brain swelling became visible at 24 h, with increased numbers of inflammatory cells that included microglia, astrocytes, and neutrophils. Brain swelling and tissue necrosis were more evident at 48 h. The hematoma started to dissolve with glial cell proliferation and new vessel formation at day 5 after ICH.

3.2. Time course of thrombin expression

Thrombin protein expression was low in the control group. In response to ICH, its expression started to increase at 3 h, was significantly increased at 10 h, and reached a maximum at day 2 (Fig. 1).

3.3. Time course of PAR-1 expression

Using immunohistochemistry, we observed that PAR-1 immunoreactivity was weak in brain sections from the control group (Fig. 2A). In hemorrhagic brain sections, perihematomal tissue showed increased PAR-1 immunoreactivity in the cytoplasm of neuron-like and glial-like cells at 2 h and 12 h after ICH (Fig. 2B, C). Using qRT-PCR, we observed that PAR-1 mRNA was significantly increased by 2 h and remained high for up to 5 days; peak levels were observed at 3 h and 2 days after ICH (Fig. 2D). Data from immunohistochemistry and Western blot experiments showed a similar trend of PAR-1 protein expression, with peaks at 3 h, 10 h, and 2 days after ICH (Table 1, Fig. 2E).

3.4. Time course of MMP-9 expression

MMP-9 immunoreactivity was weak in brain sections from the control group (Fig. 3A). In agreement with the data available in the literature, we observed a clear increase in MMP-9 immunoreactivity in brain sections from the perihematomal region. Increased MMP-9 immunoreactivity was observed mostly in neuron-like and astrocyte-like cells (Fig. 3B, C). In the perihematomal region, the number of MMP-9 immunostained cells began to increase at 2 h, remained at high levels from 3 h to 1 day, and peaked 2 days after ICH (Table 1). Western blot data showed a similar trend, with MMP-9 protein expression increasing at 3 h and reaching a maximum at day 2 after ICH (Fig. 3D).

3.5. Time course of AQP-4 expression

qRT-PCR showed that AQP-4 mRNA was upregulated beginning at 2 h, continued to increase from 3 h to 6 h, and peaked at 12 h. By 5 days post-ICH, the AQP-4 mRNA level had returned nearly to baseline (Fig. 4A). In contrast, AQP-4 protein expression began to increase by 3 h and peaked at day 5 after ICH (Fig. 4B).

3.6. Time course of brain water content

Brain water content was determined by the wet/dry weight ratio method to evaluate cerebral edema. Our results indicate that brain water content was significantly increased at 2 h and 12 h and then continued to increase, reaching a maximum at day 2 post-ICH. On day 5, the level had decreased but was still elevated compared to baseline (Fig. 5). Brain water content showed weak correlation with temporal patterns of protein expression of thrombin ($n= 5$, $r = 0.350$, $P < 0.05$) and AQP-4 ($n=5$, $r = 0.320$, $P < 0.05$) and no correlation with PAR-1 or MMP-9 expression.

4. Discussion

To our knowledge, this is the first systematic study performed to characterize the temporal profile of the expression of thrombin, PAR-1, MMP-9, and AQP-4 at the translational and/or transcriptional levels in the hemorrhagic brains of rats and to assess their potential correlation with brain edema formation. The target mRNA and/or protein expression was upregulated between 2 h and 5 days after ICH; the peak level for each was observed at 2 days, except for that of AQP-4 protein, which reached its maximum at 5 days. The time course for increases in brain water content followed a similar trend, beginning at 2 h and peaking at 2 days; the level was decreased but still elevated compared to baseline at 5 days. Brain water content showed weak correlation with temporal patterns of protein expression of thrombin and AQP-4 but no correlation with PAR-1 or MMP-9. Together, our data suggest that upregulation of these inflammatory mediators occurs as early as 2–3 h and persists for several days after ICH, and that temporal patterns of expression of thrombin and AQP-4 correlate with brain edema formation.

Available evidence indicates that thrombin contributes to ICH-induced secondary brain injury through activation of PAR-1 (Hua et al., 2007; Kitaoka et al., 2002; Ohnishi et al., 2007; Xue and Del Bigio, 2005; Xue et al., 2009b). Consistent with the results of Zheng et al. (Zheng et al., 2009), we found that thrombin and PAR-1 were upregulated concomitantly starting at 3 h and peaking 2 days post-ICH. Thrombin itself not only stimulates astrocytes and microglia (Moller et al., 2000; Noorbakhsh et al., 2003), but also directly causes neuronal death, blood-brain barrier (BBB) disruption, and brain edema formation (Lee et al., 1997; Satpathy et al., 2004; Xue and Del Bigio, 2001, 2005). Interestingly, the activation of PAR-1 also mediates thrombin-induced MMP-9 expression in rat primary astrocytes (Choi et al., 2008). Furthermore, it has been reported that thrombin and MMP-9 have a synergistic and toxic role (Xue et al., 2006). However, thrombin may play a different role during brain recovery and neurogenesis after ICH (Hua et al., 2009; Yang et al., 2008).

MMP-9 has been associated with poor ICH outcomes because of its contributions to perihematomal edema formation and neuronal death (Abilleira et al., 2003; Alvarez-Sabin et al., 2004; Castellazzi et al., 2010; Silva et al., 2005; Wang et al., 2003; Wang and Tsirka, 2005b; Xue and Yong, 2008). Two human histopathologic studies showed that, compared with the contralateral hemisphere, perihematomal tissue had higher MMP-9 activity in close relationship with neurons and glial cells (Rosell et al., 2006; Tejima et al., 2007). Here, our data demonstrated that MMP-9 immunoreactivity increases mostly in neuron-like and astrocyte-like cells in the perihematomal region starting at 3 h and reaching a maximum 2 days after ICH. This increase corresponds in time with the increase in blood MMP-9 levels seen in patients with acute ICH (Abilleira et al., 2003; Alvarez-Sabin et al., 2004; Castellazzi et al., 2010; Silva et al., 2005).

AQP-4 is the most abundant water channel protein in the brain and helps to maintain brain water homeostasis (Zador et al., 2009). Here, our data demonstrated a dynamic change in AQP-4 expression, which started to increase at 3 h and reached a maximum at day 5 after ICH. The exact role of AQP-4 in ICH is not clear. Some studies have shown AQP-4 to be detrimental. For example, AQP-4 knockout mice were reported to have decreased brain edema and better stroke outcome (Manley et al., 2000). Furthermore, after ICH, a decrease in brain edema conferred by the iron chelator deferoxamine or the thrombin inhibitor hirudin was correlated with AQP-4 inhibition (Qing et al., 2009; Sun et al., 2009). However, in another study that used AQP-4 knockout mice, Tang et al. (Tang et al., 2010) reported a protective role of activated AQP-4 after ICH.

In ICH, perihematomal edema formation is initiated partially by clot-derived proteins and vasoactive substances that disrupt BBB integrity. Thrombin, PAR-1, MMPs, and AQP-4 have been suggested to play a role in this process [reviewed in (Wang and Doré, 2007b; Wang and Tsirka, 2005a; Xi et al., 2006; Zador et al., 2009)]. Although the specific role of the selected inflammatory markers in ICH pathology is not totally clear, different temporal patterns of upregulation suggest different roles in secondary brain damage. In agreement with their potential role in ICH pathology, we observed a weak correlation over time between the brain water content and the protein expression of thrombin and AQP-4, further supporting their contribution in brain edema formation after ICH.

In terms of experimental limitations, we recognize that there is a need to extend our present study by conducting double immunofluorescence labeling to localize the described target proteins to specific cell types. Moreover, this study does not directly address the specific contribution of these inflammatory mediators to edema formation after ICH. One possibility is that ICH-related clotting activates thrombin, which, through its receptor PAR-1, activates MMP-9 and AQP-4; MMP-9 and AQP-4 then modulate the BBB integrity and edema formation. Of course, this proposed hypothesis and the efficacy of intervention with anti-inflammatory drugs need to be confirmed in future studies.

In conclusion, our data provide novel evidence that upregulation of thrombin, PAR-1, MMP-9, and AQP-4 occurs very early and persists for several days after ICH and that temporal patterns of expression of thrombin and AQP-4 are correlated with brain edema formation. These findings have implications for efforts to reduce ICH-induced secondary brain damage and to develop anti-inflammatory strategies to treat ICH patients.

Acknowledgments

This work was supported by the Natural Science Foundation of Heilongjiang Province ZJY0705 and the Foundation of the First Clinical Hospital of Harbin Medical University Y08-009 (HW) and by AHA 09BGIA2080137 and NIH K01AG031926 (JW). We thank Claire Levine for assistance with this manuscript.

References

Abilleira S, Montaner J, Molina CA, Monasterio J, Castillo J, Alvarez-Sabin J. Matrix metalloproteinase-9 concentration after spontaneous intracerebral hemorrhage. J Neurosurg 2003;99:65–70. [PubMed: 12854746]

Alvarez-Sabin J, Delgado P, Abilleira S, Molina CA, Arenillas J, Ribo M, Santamarina E, Quintana M, Monasterio J, Montaner J. Temporal profile of matrix metalloproteinases and their inhibitors after spontaneous intracerebral hemorrhage: relationship to clinical and radiological outcome. Stroke 2004;35:1316–1322. [PubMed: 15087562]

Castellazzi M, Tamborino C, De Santis G, Garofano F, Lupato A, Ramponi V, Trentini A, Casetta I, Bellini T, Fainardi E. Timing of serum active MMP-9 and MMP-2 levels in acute and subacute phases after spontaneous intracerebral hemorrhage. Acta Neurochir Suppl 2010;106:137–140. [PubMed: 19812936]

Choi MS, Kim YE, Lee WJ, Choi JW, Park GH, Kim SD, Jeon SJ, Go HS, Shin SM, Kim WK, Shin CY, Ko KH. Activation of protease-activated receptor1 mediates induction of matrix metalloproteinase-9 by thrombin in rat primary astrocytes. Brain Res Bull 2008;76:368–375. [PubMed: 18502312]

Hua Y, Keep RF, Gu Y, Xi G. Thrombin and brain recovery after intracerebral hemorrhage. Stroke 2009;40:S88–89. [PubMed: 19064789]

Hua Y, Keep RF, Hoff JT, Xi G. Brain injury after intracerebral hemorrhage: the role of thrombin and iron. Stroke 2007;38:759–762. [PubMed: 17261733]

Kitaoka T, Hua Y, Xi G, Hoff JT, Keep RF. Delayed argatroban treatment reduces edema in a rat model of intracerebral hemorrhage. Stroke 2002;33:3012–3018. [PubMed: 12468805]

Lee KR, Kawai N, Kim S, Sagher O, Hoff JT. Mechanisms of edema formation after intracerebral hemorrhage: effects of thrombin on cerebral blood flow, blood-brain barrier permeability, and cell survival in a rat model. J Neurosurg 1997;86:272–278. [PubMed: 9010429]

Manley GT, Fujimura M, Ma T, Noshita N, Filiz F, Bollen AW, Chan P, Verkman AS. Aquaporin-4 deletion in mice reduces brain edema after acute water intoxication and ischemic stroke. Nat Med 2000;6:159–163. [PubMed: 10655103]

Moller T, Hanisch UK, Ransom BR. Thrombin-induced activation of cultured rodent microglia. J Neurochem 2000;75:1539–1547. [PubMed: 10987834]

Noorbakhsh F, Vergnolle N, Hollenberg MD, Power C. Proteinase-activated receptors in the nervous system. Nat Rev Neurosci 2003;4:981–990. [PubMed: 14682360]

Ohnishi M, Katsuki H, Fujimoto S, Takagi M, Kume T, Akaike A. Involvement of thrombin and mitogen-activated protein kinase pathways in hemorrhagic brain injury. Exp Neurol 2007;206:43–52. [PubMed: 17498698]

Qing WG, Dong YQ, Ping TQ, Lai LG, Fang LD, Min HW, Xia L, Heng PY. Brain edema after intracerebral hemorrhage in rats: the role of iron overload and aquaporin 4. J Neurosurg 2009;110:462–468. [PubMed: 19025353]

Rosell A, Ortega-Aznar A, Alvarez-Sabin J, Fernandez-Cadenas I, Ribo M, Molina CA, Lo EH, Montaner J. Increased brain expression of matrix metalloproteinase-9 after ischemic and hemorrhagic human stroke. Stroke 2006;37:1399–1406. [PubMed: 16690896]

Rosenberg GA, Navratil M. Metalloproteinase inhibition blocks edema in intracerebral hemorrhage in the rat. Neurology 1997;48:921–926. [PubMed: 9109878]

Satpathy M, Gallagher P, Lizotte-Waniewski M, Srinivas SP. Thrombin-induced phosphorylation of the regulatory light chain of myosin II in cultured bovine corneal endothelial cells. Exp Eye Res 2004;79:477–486. [PubMed: 15381032]

Silva Y, Leira R, Tejada J, Lainez JM, Castillo J, Davalos A. Molecular signatures of vascular injury are associated with early growth of intracerebral hemorrhage. Stroke 2005;36:86–91. [PubMed: 15550687]

Sun Z, Zhao Z, Zhao S, Sheng Y, Zhao Z, Gao C, Li J, Liu X. Recombinant hirudin treatment modulates aquaporin-4 and aquaporin-9 expression after intracerebral hemorrhage in vivo. Mol Biol Rep 2009;36:1119–1127. [PubMed: 18574711]

Tang Y, Wu P, Su J, Xiang J, Cai D, Dong Q. Effects of Aquaporin-4 on edema formation following intracerebral hemorrhage. Exp Neurol. 2010 In press.

Tejima E, Zhao BQ, Tsuji K, Rosell A, van Leyen K, Gonzalez RG, Montaner J, Wang X, Lo EH. Astrocytic induction of matrix metalloproteinase-9 and edema in brain hemorrhage. J Cereb Blood Flow Metab 2007;27:460–468. [PubMed: 16788715]

Wang J, Doré S. Heme oxygenase-1 exacerbates early brain injury after intracerebral haemorrhage. Brain 2007a;130:1643–1652. [PubMed: 17525142]

Wang J, Doré S. Inflammation after intracerebral hemorrhage. J Cereb Blood Flow Metab 2007b; 27:894–908. [PubMed: 17033693]

Wang J, Rogove AD, Tsirka AE, Tsirka SE. Protective role of tuftsin fragment 1-3 in an animal model of intracerebral hemorrhage. Ann Neurol 2003;54:655–664. [PubMed: 14595655]

Wang J, Tsirka SE. Contribution of extracellular proteolysis and microglia to intracerebral hemorrhage. Neurocrit Care 2005a;3:77–85. [PubMed: 16159103]

Wang J, Tsirka SE. Neuroprotection by inhibition of matrix metalloproteinases in a mouse model of intracerebral haemorrhage. Brain 2005b;128:1622–1633. [PubMed: 15800021]

Wu H, Zhao R, Qi J, Cong Y, Wang D, Liu T, Gu Y, Ban X, Huang Q. The expression and the role of protease nexin-1 on brain edema after intracerebral hemorrhage. J Neurol Sci 2008;270:172–183. [PubMed: 18442833]

Xi G, Keep RF, Hoff JT. Mechanisms of brain injury after intracerebral haemorrhage. Lancet Neurol 2006;5:53–63. [PubMed: 16361023]

Xi G, Reiser G, Keep RF. The role of thrombin and thrombin receptors in ischemic, hemorrhagic and traumatic brain injury: deleterious or protective? J Neurochem 2003;84:3–9. [PubMed: 12485396]

Xue M, Del Bigio MR. Acute tissue damage after injections of thrombin and plasmin into rat striatum. Stroke 2001;32:2164–2169. [PubMed: 11546912]

Xue M, Del Bigio MR. Injections of blood, thrombin, and plasminogen more severely damage neonatal mouse brain than mature mouse brain. Brain Pathol 2005;15:273–280. [PubMed: 16389939]

Xue M, Fan Y, Liu S, Zygun DA, Demchuk A, Yong VW. Contributions of multiple proteases to neurotoxicity in a mouse model of intracerebral haemorrhage. Brain 2009a;132:26–36. [PubMed: 18772219]

Xue M, Hollenberg MD, Demchuk A, Yong VW. Relative importance of proteinase-activated receptor-1 versus matrix metalloproteinases in intracerebral hemorrhage-mediated neurotoxicity in mice. Stroke 2009b;40:2199–2204. [PubMed: 19359644]

Xue M, Hollenberg MD, Yong VW. Combination of thrombin and matrix metalloproteinase-9 exacerbates neurotoxicity in cell culture and intracerebral hemorrhage in mice. J Neurosci 2006;26:10281–10291. [PubMed: 17021183]

Xue M, Yong VW. Matrix metalloproteinases in intracerebral hemorrhage. Neurol Res 2008;30:775–782. [PubMed: 18826803]

Yang S, Song S, Hua Y, Nakamura T, Keep RF, Xi G. Effects of thrombin on neurogenesis after intracerebral hemorrhage. Stroke 2008;39:2079–2084. [PubMed: 18436875]

Zador Z, Stiver S, Wang V, Manley GT. Role of aquaporin-4 in cerebral edema and stroke. Handb Exp Pharmacol 2009:159–170. [PubMed: 19096776]

Zheng GQ, Wang XT, Wang XM, Gao RR, Zeng XL, Fu XL, Wang Y. Long-time course of protease-activated receptor-1 expression after intracerebral hemorrhage in rats. Neurosci Lett 2009;459:62–65. [PubMed: 19427359]

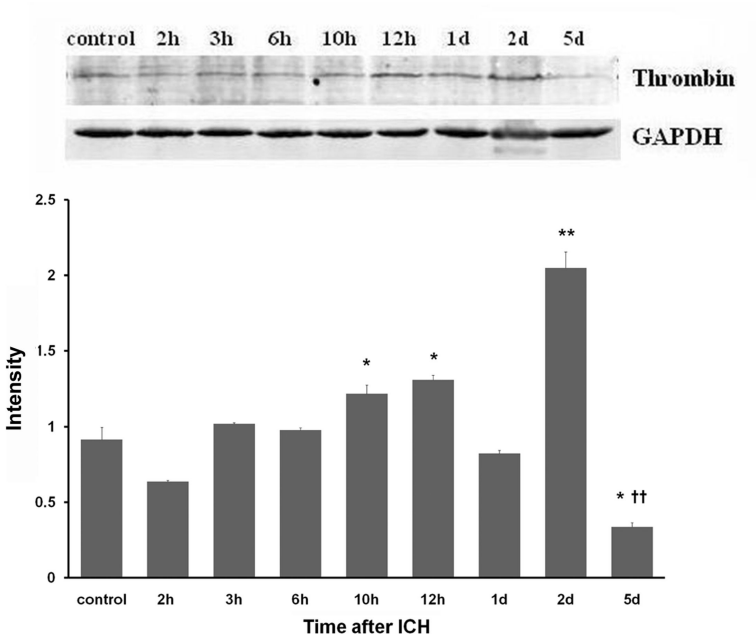

Fig. 1.

Thrombin protein expression after ICH in rat brain. ICH rats were infused with 50 μL of autologous whole blood; control rats were infused with an equal volume of saline. Western blot analysis showed that expression of thrombin started to increase at 3 h after blood injection, significantly increased at 10–12 h, and peaked at day 2 after ICH. GAPDH was used as a loading control. Intensities (means ± SD) were normalized to their respective control (n=5/group). Experiments were performed in triplicate with similar results. **P*<0.05, ***P*<0.01 compared with the control group. ††*P*<0.01 compared with the previous time point.

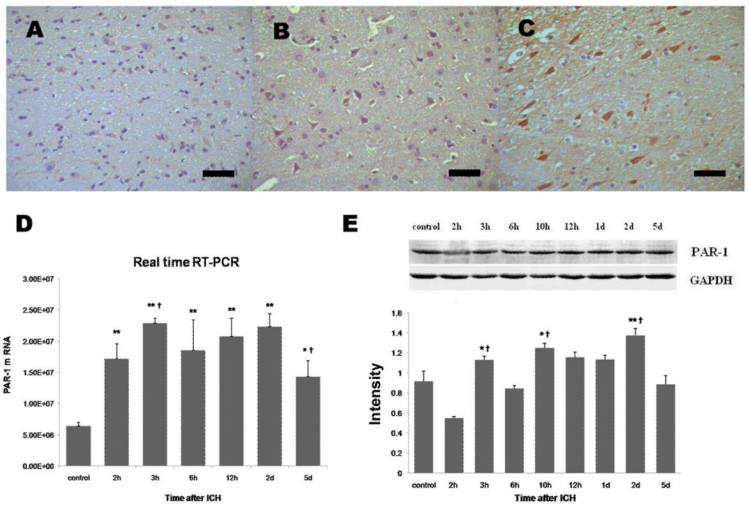

Fig. 2.

PAR-1 mRNA and protein expression after ICH in rat brain. ICH rats were infused with 50 μL of autologous whole blood; control rats were infused with an equal volume of saline. (A) Immunohistochemistry showed that PAR-1 immunoreactivity was mild in brain sections from the control group. PAR-1 immunoreactivity was increased in the perihematomal region at 2 h (B) and further increased at 12 h (C). Scale bar = 100 μm. (D) Real-time quantitative RT-PCR analysis showed that PAR-1 mRNA was significantly elevated compared to control from 2 h through at least 5 days post-ICH. The mRNA level is expressed in arbitrary units. (E) Western blot analysis showed that PAR-1 protein expression was significantly elevated at 3 h, 10 h, and 2 days after ICH. GAPDH was used as a loading control. Intensities (means ± SD) were normalized to their respective control (n=5/group). Immunoblotting was performed in triplicate with similar results. *P<0.05, **P<0.01 compared with the control group. †P<0.05 compared with the previous time point.

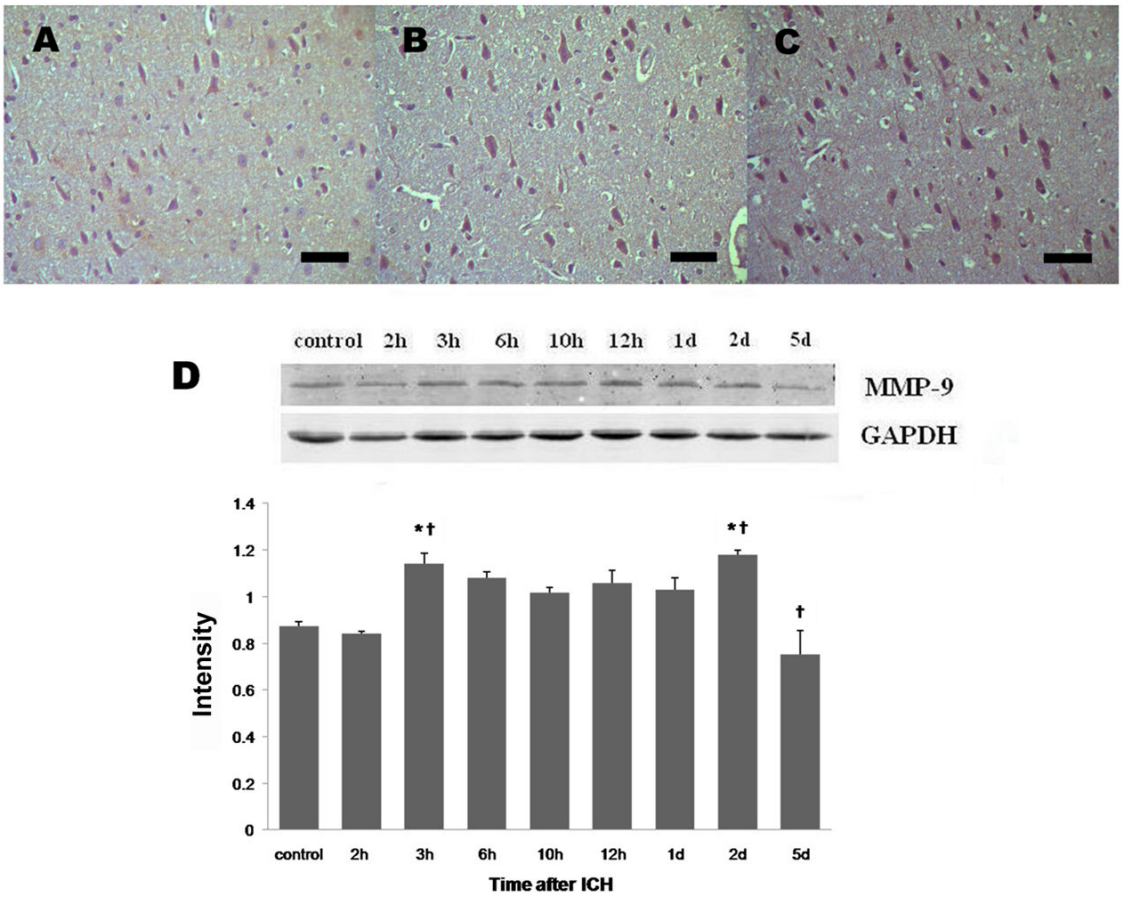

Fig. 3.

MMP-9 protein expression after ICH in rat brain. ICH rats were infused with 50 μL of autologous whole blood; control rats were infused with an equal volume of saline. (A) Immunohistochemistry showed that MMP-9 immunoreactivity was mild in brain sections from the control group. MMP-9 immunoreactivity was increased in the perihematomal region at 2 h (B) and further increased 2 days after ICH (C). Scale bar = 100 μm. (D) Western blot analysis showed that MMP-9 protein expression was significantly increased at 3 h and 2 days after ICH. GAPDH was used as a loading control. Intensities (means ± SD) were normalized to their respective control (n=5/group). Immunoblotting was performed in triplicate with similar results. **P*<0.05 compared with the control group. †*P*<0.05 compared with the previous time point.

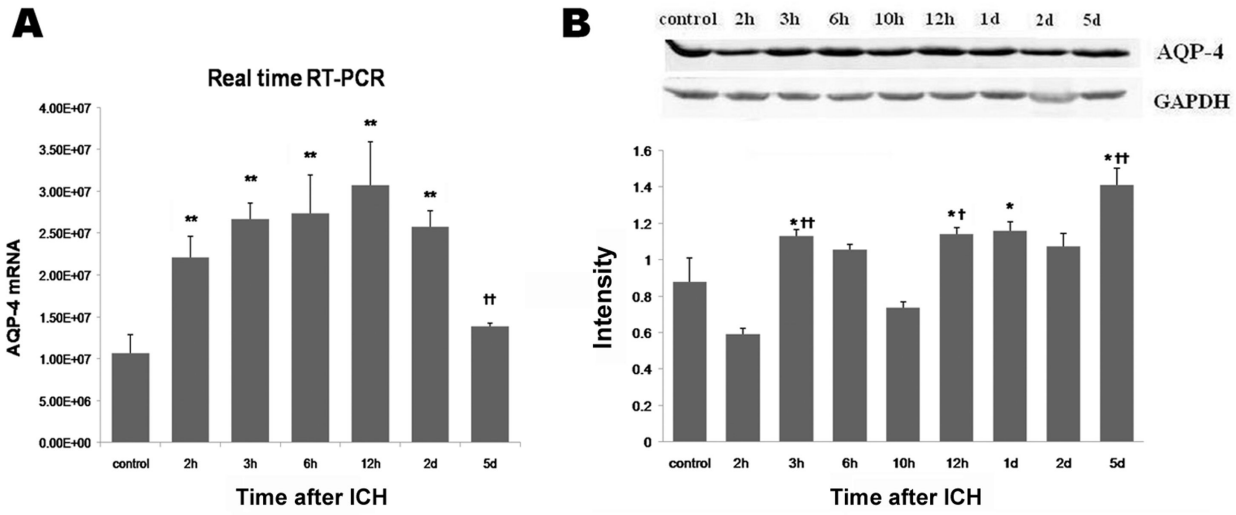

Fig. 4.

AQP-4 mRNA and protein expression after ICH in rat brain. ICH rats were infused with 50 μL of autologous whole blood; control rats were infused with an equal volume of saline. (A) Real-time quantitative RT-PCR analysis showed that AQP-4 mRNA was significantly increased by 2 h, peaked at 12 h, and began to decrease at day 2 after ICH. The mRNA level is expressed in arbitrary units. (B) Western blot analysis showed that AQP-4 protein expression increased at 3 h, declined at 10 h, and then increased again, reaching a peak 5 days after ICH. GAPDH was used as a loading control. Intensities (means ± SD) were normalized to their respective control (n=5/group). Immunoblotting was performed in triplicate with similar results. **P*<0.05, ***P*<0.01 compared with the control group. †*P*<0.05, ††*P*<0.01 compared with the previous time point.

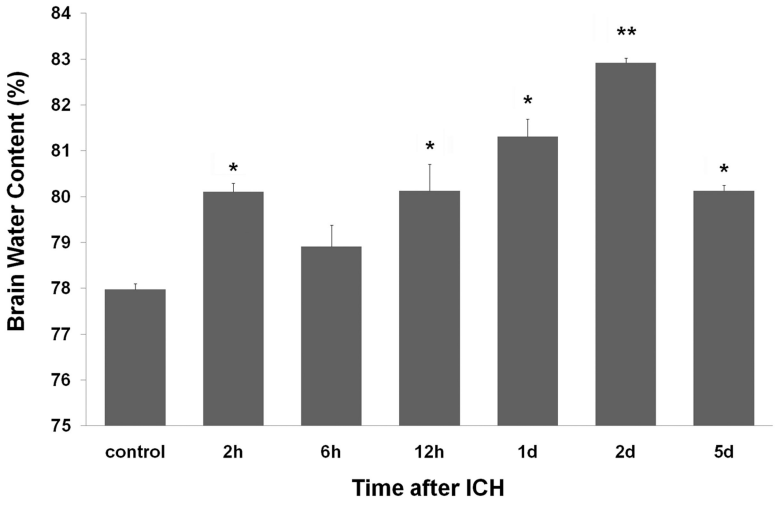

Fig. 5.

Brain water content after ICH in rat brain. Using the wet/dry weight ratio method, our results showed that brain water content began to increase at 2 h, further increased at 12 h and 1 day, peaked at day 2, and decreased at day 5 after ICH. Values are means ± SD (n=5/group). *P<0.05, **P<0.01 compared with the control group.

Table 1

Immunoreactivity of PAR-1 and MMP-9 in rat brain after intracerebral hemorrhage

Group	Number of immunostained cells per 40x field	
	PAR-1	MMP-9
Control	82.6±12.0	89.8±24.0
2 h	110.8±47.2	142.3±44.7**††
3 h	138.2±37.0**†	153±44.8**
6 h	116.6±20.7*	137.6±21.5**
10 h	139.9±44.6**	124.3±25.2
12 h	153.8±23.8**	152.4±33.6**†
1 d	102.8±25.3††	116.5±36.7†
2 d	143.3±15.9**††	167.5±43.8**††
5 d	119.3±19.5†	120±16.8††

Experimental rats were infused with 50 μL of autologous whole blood; control rats were infused with an equal volume of saline. Data are mean ± SD; n = 5 rats per group.

$^{*}P<0.05$

$^{**}P<0.01$ compared with the control group.

$^{\dagger}P<0.05$

$^{\dagger\dagger}P<0.01$ compared with the previous time point.